

1 A forced Korteweg-de Vries model for nonlinear mixing of oscillations in a dusty 2 plasma

3 Ajaz A. Mir,¹ Sanat K. Tiwari,^{1,*} John Goree,² Abhijit Sen,³ Chris Crabtree,⁴ and Gurudas Ganguli⁴

4 ¹Indian Institute of Technology Jammu, Jammu, J&K, 181221, India

5 ²Department of Physics and Astronomy, University of Iowa, Iowa City, IA 52242, USA

6 ³Institute for Plasma Research, Gandhinagar, Gujarat, 382428, India

7 ⁴Naval Research Laboratory, Washington, DC 20375, USA

8 (Dated: September 18, 2020)

9 Nonlinear mixing of oscillations in a dusty plasma due to the harmonic time varying modulation
10 of a nonlinear compressional oscillation is analyzed using a simple mathematical model consisting
11 of a forced Korteweg-de Vries equation. An exact analytic solution of this equation is found to
12 exhibit nonlinear mixing in the system. The model solution can be usefully employed to predict
13 the existence of nonlinear mixing of oscillations in a two-dimensional dusty plasma system of a
14 particular experimental configuration.

15 I. INTRODUCTION

16 Nonlinear mixing is a phenomenon found in many
17 physical systems that can sustain waves of large ampli-
18 tudes [1–4]. In a dusty plasma, compressional waves can
19 easily attain large amplitudes, even if the electric poten-
20 tial variation is only a few millivolts, and this is due to the
21 large electric charge of thousands of elementary charges
22 [4, 5] residing on a dust particle.

23 Two kinds of compressional waves in dusty plasmas
24 are the dust-acoustic wave and the longitudinal dust lat-
25 tice wave [6–8]. The dust-acoustic wave (DAW) propa-
26 gates in a three-dimensional cloud of charged dust parti-
27 cles which are immersed in a mixture of electrons and
28 ions; all three of these charged species participate in
29 the compression and rarefaction. If there is an ambi-
30 ent steady electric field, it will drive an ion current that
31 can easily self-excite the DAW through an instability,
32 which commonly occurs in laboratory gas-discharge plas-
33 mas [9, 10]. On the other hand, the longitudinal dust
34 lattice wave (DLW) propagates in a different situation;
35 while the electrons and ions fill a three-dimensional vol-
36 ume, the dust particles do not; they are instead confined
37 to a planar layer which is thin, and often is just a mono-
38 layer. Because of the paucity of dust particles, the elec-
39 trons and ions are not significantly affected by the dust
40 particles, and for the most part they just contribute to
41 the Debye screening of the inter-particle repulsion among
42 the dust particles [6]. Unlike the DAW, the longitudinal
43 dust lattice wave is not necessarily excited by an ambient
44 DC electric field, so that in the laboratory it is common
45 to excite it by an external forcing [11, 12].

46 In this paper we consider the longitudinal dust lat-
47 tice wave, with two sinusoidal external excitations at a
48 large amplitude, to cause nonlinear mixing. By pertur-
49 bing a two-dimensional crystalline layer of dust particles
50 using two laser beams of different frequencies, three-wave
51 mixing was experimentally demonstrated by Nosenko *et*

52 *al.* [13]. In this paper, we theoretically demonstrate non-
53 linear mixing phenomenon in a dusty plasma system us-
54 ing an analytic solution of a sinusoidally forced Korteweg-
55 de Vries model equation. The model solution can also be
56 usefully employed to predict the existence of nonlinear
57 mixing in a variant of the two-dimensional experimental
58 dusty plasma experiment reported in Ref. [13].

59 In their experiment, the authors of Ref. [13] used
60 a horizontal monolayer of dust, which consisted of pre-
61 cision polymer microspheres that were levitated above
62 a lower electrode of a radio-frequency glow-discharge
63 plasma. Using video microscopy, they verified that the
64 equilibrium state of this cloud of particles was a trian-
65 gular lattice with a six-fold symmetry. The charge on
66 a microsphere was $-9400 e$ (where e is the charge of
67 an electron), the crystalline lattice constant was 675 mi-
68 crons, and the mass of the 8 micron microspheres was
69 sufficiently high that the compressional sound speed in
70 the lattice was only 22 mm/s.

71 The experimenters of Ref. [13] launched two longi-
72 tudinal lattice waves, with sinusoidal waveforms at dif-
73 ferent frequencies f_1 and f_2 . Each of these two waves
74 were propagating waves, and they were each excited ex-
75 ternally by the radiation-pressure force, using laser ma-
76 nipulation with a steady-state laser that was amplitude
77 modulated at the desired low frequency. The dust cloud
78 was a horizontal monolayer. The excitation regions for
79 the two waves were physically separate, which is a point
80 that is important for the present paper. The spatial lo-
81 calization of the excitation regions was achieved by mak-
82 ing the laser beams incident on the dust layer at an
83 angle of 10 degrees. The experimenters then observed
84 waves at various difference and sum frequencies, includ-
85 ing $f_1 + f_2$, $f_2 - f_1$, $2f_2 - f_1$, and so on. They confirmed
86 using bi-spectral analysis that these were the products
87 of nonlinear mixing. In this way, they provided an ex-
88 perimental observation of three-wave mixing, in a dusty
89 plasma.

90 The physical system in that experiment can be mod-
91 eled theoretically by several descriptions, including a
92 point-like particle description and a continuum descrip-

* sanat.tiwari@iitjammu.ac.in

This is the author's peer reviewed, accepted manuscript. However, the online version of record will be different from this version once it has been copyedited and typeset.

PLEASE CITE THIS ARTICLE AS DOI: 10.1063/5.0022482

143

II. THEORETICAL MODEL

144 Our theoretical approach relies on two basic
 145 premises - (i) nonlinear compressional waves in a dusty
 146 plasma system can be modeled by a KdV equation, and
 147 (ii) the forced KdV equation can model their dynamics

148 tion of the dust layer. The latter approach was used by
 149 Avinash *et al.* [14], who modeled the long-wavelength
 150 compressional waves in the monolayer triangular lattice,
 151 as obeying an evolution equation described by a variant
 152 of the Korteweg-de Vries (KdV) equation.

153 In this paper, we predict theoretically that nonlinear
 154 mixing can occur also in a different excitation configura-
 155 tion, where only one of the two excitation frequencies f_1
 156 has a propagating wave that is excited locally, while the
 157 other frequency f_2 is a non-localized oscillation. In both
 158 cases, the external forcing can be provided by any physi-
 159 cal force, including the radiation pressure force that was
 160 used in Ref. [13]. Unlike Ref. [13], only the frequency f_1
 161 has a propagating wave that is excited in a spatially local-
 162 ized region, and as a crucial difference, frequency f_2 has
 163 a spatially uniform force, varying sinusoidally in time but
 164 not in space. This construction should be feasible sim-
 165 ply by performing an experiment with a two-dimensional
 166 monolayer of dust as in the experiment of Ref. [13], but
 167 with one of the two laser beams incident on the particle
 168 cloud at zero degrees instead of ten degrees. A schematic
 169 sketch of the excitation configuration is shown in Fig. 1.

170 Although we are mainly concerned here with non-
 171 linear mixing of the longitudinal lattice wave, we can
 172 mention another kind of nonlinear effect which has been
 173 observed experimentally, and that is synchronization. In
 174 synchronization, there is an inherent oscillation at one
 175 frequency and an external forcing at a second frequency.
 176 The second frequency must be close to that of the in-
 177 herent oscillation, or one of its harmonics. Although
 178 synchronization has long been understood for point os-
 179 cillators, it can also occur in the more complicated case
 180 of propagating waves, and indeed it is known to occur
 181 in three-dimensional dust clouds that sustain the dust
 182 acoustic wave (DAW). The DAW is self-excited at an
 183 inherent frequency due to ion flow, and an external si-
 184 nusoidal forcing can be applied for example by a vol-
 185 tage applied to the entire cloud by an electrode so that
 186 the entire cloud experiences a global modulation [15, 16].
 187 The result of synchronization is that the inherent oscil-
 188 lation is shifted in its frequency, for example to match
 189 the frequency of the external forcing. This is different
 190 from the case of mixing, where the two original waves
 191 maintain their frequencies and a third wave appears at
 192 yet another frequency. Another distinction, in comparing
 193 synchronization and mixing, is that the original two oscil-
 194 lations can have frequencies that differ greatly in the case
 195 of mixing, whereas for synchronization it is necessary for
 196 there to be a small difference in the two frequencies or
 197 their harmonics.

198 in the presence of an external driving force. For a three-
 199 dimensional dust cloud, the KdV equation as a model
 200 description of nonlinear DAWs is well established. It was
 201 first derived by Rao *et al.* [17] using a fluid represen-
 202 tation of the dusty plasma and has subsequently been
 203 widely used in many theoretical and experimental stud-
 204 ies [4, 18–20]. An fKdV model, within the fluid prescrip-
 205 tion, was first derived by Sen *et al.* [21] for describing
 206 driven nonlinear ion acoustic waves. The generic form of
 207 this model equation was subsequently shown to apply for
 208 driven DAWs as well and was successfully used to inter-
 209 pret the excitation of precursor dust acoustic solitons in
 210 a laboratory dusty plasma device [22, 23].

211 For the dust lattice wave, the KdV model has also
 212 been shown by Farokhi *et al.* [24] to theoretically describe
 213 the nonlinear evolution of waves in a two-dimensional
 214 dust lattice system. Thus one can expect the fKdV
 215 model to also successfully describe the dynamics of driven
 216 DLWs in the case of a two-dimensional lattice system
 217 subject to external forcing.

218 Hence as a paradigmatic model for driven compres-
 219 sional nonlinear oscillations in a dusty plasma system we
 220 adopt the generic fKdV equation given as,

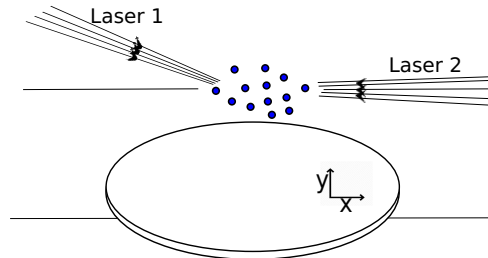


FIG. 1. A cartoon representation of a proposed experimental configuration with one of the laser beams incident on the dust at zero degrees to provide a non-localized driving oscillation. Thousands of charged dust particles, shown schematically here as a few dots, are levitated in a single horizontal layer in an electric sheath above a powered lower electrode, shown schematically as a disk at the bottom of this diagram.

$$171 \frac{\partial n(x, t)}{\partial t} + \alpha n(x, t) \frac{\partial n(x, t)}{\partial x} + \beta \frac{\partial^3 n(x, t)}{\partial x^3} = F_s(x, t) \quad (1)$$

172 where n is a perturbed physical quantity (representing
 173 the perturbed dust density for example) and $F_s(x, t)$ is
 174 the driving source term. The coefficients α and β rep-
 175 resent the strengths of the nonlinear and dispersive con-
 176 tributions, respectively. Dissipative effects, such as may
 177 occur due to frictional damping from neutral gas parti-
 178 cles, are not included in this model, so that it cannot
 179 describe phenomena such as synchronization that need
 180 dissipation. For $F_s(x, t) = 0$, Eq. (1) represents the
 181 standard KdV equation that has been extensively stud-
 182 ied in the past to describe nonlinear wave propagation

183 in neutral fluids [25], plasmas [26, 27], dusty plasmas
 184 [14, 17, 19, 28, 29] and other nonlinear dispersive media
 185 [30, 31].

186 The KdV equation has a variety of solutions includ-
 187 ing solitons and cnoidal wave solutions. The latter are
 188 relevant for our present work and are given by [32, 33]

$$189 \quad n(x, t) = \mu \operatorname{cn}^2 \left[\frac{\sqrt{\mu\alpha}}{2\sqrt{\beta\kappa(\kappa+2)}} \xi(x, t); \kappa \right] \quad (2)$$

190 with

$$191 \quad \xi(x, t) = \left(x - \frac{\kappa + \kappa^2 - 1}{\kappa(\kappa + 2)} \alpha \mu t \right) \quad (3)$$

192 where cn is a Jacobi elliptic function. The parameter
 193 μ represents the amplitude, which can be chosen to be
 194 any value (for example, in an experiment by adjusting
 195 the amplitude of an external forcing). The elliptic pa-
 196 rameter κ indicates the response of the medium to that
 197 amplitude. The value of the parameter κ determines
 198 the shape of the cnoidal function so that it serves as a
 199 quantitative measure of nonlinearity. For $\kappa = 0$, which
 200 is the linear case, the cnoidal solution becomes a cosine
 201 function, while for the highly nonlinear case of values
 202 close to unity, the wave form has sharp peaks and flat-
 203 tened bottoms. The cnoidal solution, Eq. (2), was re-
 204 cently shown to provide an excellent fit to experimental
 205 observations of spontaneously generated nonlinear DAWs
 206 in a three-dimensional dusty plasma cloud sustained in a
 207 RF discharge plasma [4].

208 The spatial wave length λ and frequency f_1 of the
 209 periodic wave, Eq. (2), are given by

$$210 \quad \lambda = 4K(\kappa) \sqrt{\frac{\beta(2\kappa + \kappa^2)}{\alpha\mu}} \quad (4)$$

$$211 \quad f_1 = \frac{\beta}{4K(\kappa)} (\kappa^2 + \kappa - 1) \left(\frac{\alpha\mu}{\beta(2\kappa + \kappa^2)} \right)^{3/2} \quad (5)$$

212 Here, $K(\kappa)$ is the complete elliptical integral of first kind.
 213 Expressions for the wavelength λ and frequency f_1 are
 214 obtained by comparing Eq. (2) with the following form
 215 of the solution by Dingemans *et al.* [34] and Liu *et al.*
 216 [4]

$$217 \quad n(x, t) = \mu \operatorname{cn}^2 \left[2K(\kappa) \left(\frac{x}{\lambda} - f_1 t \right); \kappa \right]. \quad (6)$$

218 To illustrate the nature of the solution, Eq. (2), and
 219 its spectral properties we will choose $\alpha = \beta = 1$ and plot
 220 the solution for several values of κ and μ . In Fig. 2(a) we
 221 plot the time series obtained from Eq. (2) at a fixed value
 222 of x for $\mu = 0.0318$ and $\kappa = 0.001$ (such that $f_1 = 10$
 223 Hz). The corresponding frequency spectrum is shown
 224 in Fig. 2(b). For this low value of κ , the wave form is
 225 approximately sinusoidal and shows a single dominant
 226 frequency $f_1 = 10$ Hz in the spectrum. A small peak
 227 at $2f_1$ due to the nonzero nonlinearity ($\kappa \neq 0$) is also
 228 observed. For a higher value of $\kappa = 0.8$ and $\mu = 78$ (such

229 that f_1 is still 10 Hz) the wave form is more nonlinear
 230 in character, as shown in Fig. 2(c), and the spectrum
 231 Fig. 2(d) shows the appearance of higher harmonics at
 232 $2f_1, 3f_1$ etc.

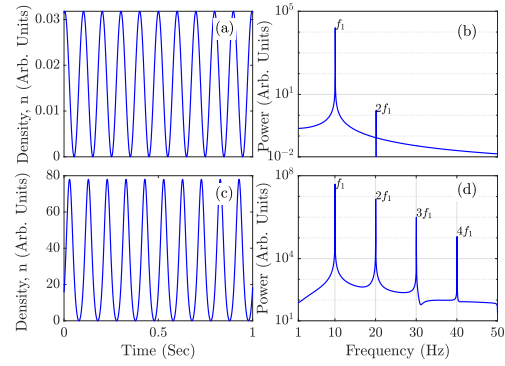


FIG. 2. Time series and the corresponding power spectra for an arbitrary spontaneous density perturbation, n , as given by Eq. (2). (a) Sinusoidal-like wave with $\kappa = 0.001$, $\mu = 0.0318$ such that $f_1 = 10$ Hz. (b) Power spectrum of (a). (c) Nonlinear wave form with $\kappa = 0.8$, $\mu = 78$ and $f_1 = 10$ Hz. (d) Power spectrum of (c).

III. EXACT NONLINEAR SOLUTION AND NONLINEAR WAVE MIXING

235 We next examine the solution of the fKdV model
 236 equation, Eq. (1), with a specific form of the driving
 237 term. For a sinusoidally time varying driver, $F_s(x, t) =$
 238 $A_s \sin(2\pi f_2 t)$, Eq. (1) has an exact analytic solution (de-
 239 rived using Hirota's method as in Salas *et al.* [35]) given
 240 by

$$243 \quad n(x, t) = -\frac{A_s \cos(2\pi f_2 t)}{2\pi f_2} + \mu \operatorname{cn}^2 \left[\frac{\sqrt{\mu\alpha}}{2\sqrt{\beta\kappa(\kappa+2)}} \eta(x, t); \kappa \right]$$

$$244 \quad \eta(x, t) = \left(x - \frac{\kappa + \kappa^2 - 1}{\kappa(\kappa + 2)} \alpha \mu t + \frac{A_s \alpha}{(2\pi f_2)^2} \sin(2\pi f_2 t) \right). \quad (7)$$

247 To explore the phenomenon of wave mixing in vari-
 248 ous nonlinear regimes, we will use this exact solution for
 249 different values of the parameters, κ and μ . Now that we
 250 are driving not only at frequency f_1 , but also at frequency
 251 f_2 , we see a modulation in the time series of Fig. 3(a) and
 252 3(c), obtained from Eq. (7). The corresponding spectra
 253 are shown in Fig. 3(b) and 3(d), respectively. The con-
 254 ditions are for a weakly nonlinear amplitude in Fig. 3(a)
 255 and 3(c), with $\mu = 0.0318$, $\kappa = 0.001$ and $A_s = 0.318$.
 256 The amplitude is greater and more nonlinear in Fig. 3(b)
 257 and 3(d), with $\mu = 78$, $\kappa = 0.8$ and $A_s = 780$. In all cases

This is the author's peer reviewed, accepted manuscript. However, the online version of record will be different from this version once it has been copyedited and typeset.

PLEASE CITE THIS ARTICLE AS DOI: 10.1063/5.0022482

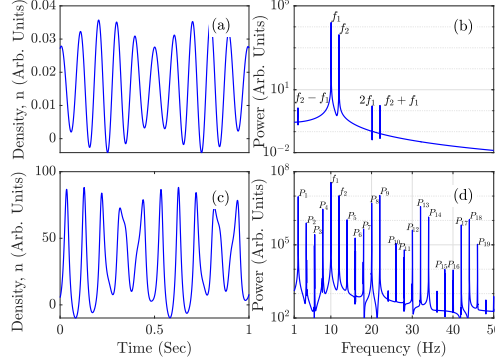


FIG. 3. Time series and the corresponding power spectra for a density perturbation, n , driven at $f_2 = 12$ Hz from Eq. (7). (a) Time series with weak nonlinearity ($\kappa = 0.001$, $\mu = 0.0318$, $f_1 = 10$ Hz, $A_s = 0.318$) and (b) the corresponding power spectra showing f_1 , f_2 and their sum and difference frequencies. (c) Time series with large nonlinearity ($\kappa = 0.8$, $\mu = 78$, $f_1 = 10$ Hz, $A_s = 780$) and (d) its corresponding power spectra showing f_1 , f_2 , their sum and difference frequencies and their harmonics.

for Fig. 3, $f_1 = 10$ Hz, $f_2 = 12$ Hz, and $\alpha = \beta = 1$. The spectrum shows peaks at f_1 , f_2 , sum-frequency $f_2 + f_1$ and difference-frequency $f_2 - f_1$.

Nonlinear mixing is revealed by the presence of combination frequencies in the spectra of Fig. 3. Especially in Fig. 3(d) with the higher nonlinearity, we see many combination frequencies such as $2f_2 - f_1$ which is labeled as peak P_5 , and $2f_1 + f_2$ which is labeled as peak P_{13} . There is a rich variety of these combination frequencies, and they are listed in Table I. The presence of peaks at harmonics such as $2f_1$, $3f_1$ and $4f_1$ are not attributed to mixing, but rather just the presence of nonlinearity ($\kappa > 0$) in the excitation.

TABLE I. Dominant frequencies observed in the spectral data shown in Fig. 3(d).

f_1	10	f_2	12
P_1	$f_2 - f_1$	P_{11}	$4f_2 - 2f_1$
P_2	$2(f_2 - f_1)$	P_{12}	$3f_1$
P_3	$3(f_2 - f_1)$	P_{13}	$2f_1 + f_2$
P_4	$4(f_2 - f_1)$	P_{14}	$2f_2 + f_1$
P_5	$2f_2 - f_1$	P_{15}	$4f_2 - f_1$
P_6	$3f_2 - 2f_1$	P_{16}	$4f_1$
P_7	$4f_2 - 3f_1$	P_{17}	$3f_1 + f_2$
P_8	$2f_1$	P_{18}	$2(f_1 + f_2)$
P_9	$f_2 + f_1$	P_{19}	$f_1 + 3f_2$
P_{10}	$3f_2 - f_1$		

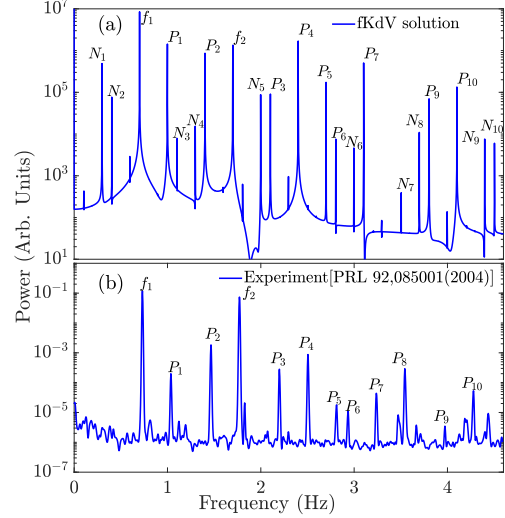


FIG. 4. Comparison of time series power spectra for [a] obtained from the fKdV model, Eq. (7), and [b] we have replotted the same experimental data points that were originally reported in Ref. [13]. Parameters used for the theoretical model are $\mu = 18.5$, $\kappa = 0.7$ (corresponds to $f_1 = 0.7$ Hz), $A_s = 18.5$ and $f_2 = 1.7$ Hz.

IV. DISCUSSION

As a specimen to illustrate a spectrum that is known to exhibit nonlinear mixing, we have replotted in Fig. 4(b) the experimental spectrum from Ref. [13]. This experimental spectrum includes peaks at combination frequencies such as $2f_2 - f_1$ and $2f_1 + f_2$. (The experiment also has peaks at harmonics such as $2f_1$ and $3f_1$, but those can occur in the absence of mixing due to the non-sinusoidal distortion of a periodic waveform, as is common under nonlinear effects.)

It is significant that the spectrum from our solution of the fKdV equation shows peaks at the same combination frequencies as for the experiment of Ref. [13]. This observation gives us some confidence that we are observing nonlinear mixing. The model, even though it is simple, adequately captures salient mechanisms for nonlinear mixing, yielding the same signatures of combination frequencies as in a specimen experimental system.

Although for Fig. 4(a) we used the same excitation frequencies $f_1 = 0.7$ Hz and $f_2 = 1.7$ Hz as for the experiment of Ref. [13], we should mention several ways that the model's assumptions differ from that of experiment. First, there is frictional damping from gas in the experiment. This friction can inhibit nonlinear effects, unless a threshold is exceeded, which would not be the case in the model where there was no friction. Second,

This is the author's peer reviewed, accepted manuscript. However, the online version of record will be different from this version once it has been copyedited and typeset.

PLEASE CITE THIS ARTICLE AS DOI: 10.1063/5.0022482

TABLE II. Frequencies observed in Fig. 4.

Frequency (Hz)	Fig. 4(a)	Fig. 4(b)
f_1	0.7	0.7
f_2	1.7	1.7
$P_1 = f_2 - f_1$	✓	✓
$P_2 = 2f_1$	✓	✓
$P_3 = 3f_1$	✓	✓
$P_4 = f_1 + f_2$	✓	✓
$P_5 = 2f_2 - f_1$	✓	✓
$P_6 = 4f_1$	✓	✓
$P_7 = 2f_1 + f_2$	✓	✓
$P_8 = 2f_2$		✓
$P_9 = 3f_1 + f_2$	✓	✓
$P_{10} = 2f_2 + f_1$	✓	✓
$N_1 = f_2 - 2f_1$	✓	
$N_2 = 3f_1 - f_2$	✓	
$N_3 = 4f_1 - f_2$	✓	
$N_4 = 2f_2 - 3f_1$	✓	
$N_5 = 2(f_2 - f_1)$	✓	
$N_6 = 3(f_2 - f_1)$	✓	
$N_7 = 5f_1$	✓	
$N_8 = 3f_2 - 2f_1$	✓	
$N_9 = 3f_2 - f_1$	✓	
$N_{10} = 4f_1 + f_2$	✓	

the experimental system was finite in size and could exhibit an overall sloshing mode oscillation in the presence of the external confining potential, which is provided by a curved sheath above the horizontal electrode. Thus, the experimental spectrum could potentially include the signature of a sloshing mode oscillation, or the mixing of that oscillation with the excitation at f_1 or f_2 . This behavior would not be described by our model. Third, the model was constructed so that it assumes that the excitation at one of the two frequencies is not a propagating wave, but is uniformly applied throughout the medium, as sketched in Fig. 1. This third difference might be less substantial than one might expect, however, because the wavelength at the low frequency $f_1 = 0.7$ Hz in the experiment could have been substantial as compared to the finite size of the cloud of charged dust particles.

We also note that the spectral peaks obtained from the theoretical fKdV model in Fig. 4(a) are not limited to all those present in the experimental spectrum shown

in Fig. 4(b). In Table II, we list those peaks P_1-P_{10} of the theoretical model that are also present in the experimental spectrum while peaks N_1-N_{10} are only present in the theoretical model. The latter frequency peaks represent different combinations of the sum and difference of f_1 , f_2 and their higher harmonics. Their absence in the experimental spectrum could be due to the effect of gas friction, which can prevent weak nonlinear effects from being observed.

V. CONCLUSIONS

To conclude, we have presented a simple mathematical model consisting of a forced KdV equation with a time varying sinusoidal forcing term that shows the existence of nonlinear wave mixing in a dusty plasma medium. Physically the model represents wave mixing arising from the temporal modulation of a nonlinear dust compressional wave. This is a situation that can be easily realized in an experiment using radiation pressure of lasers or time varying electric potentials to modulate self-excited or externally driven large amplitude compressional waves.

One advantage of the present model is the existence of an exact analytic solution which can be conveniently used to map various parametric regimes without recourse to a numerical solution of the nonlinear equation. This solution not only shows the existence of wave mixing phenomenon in this simple model system but may also be useful in predicting nonlinear wave mixing for a proposed experimental configuration in a two-dimensional dusty plasma medium.

ACKNOWLEDGMENTS

Work done by ST and AM was supported by IIT Jammu seed grant No. SG0012. JG acknowledges NASA-JPL subcontract No. 1573629 and U.S. DOE grant DE-SC0014566. CC and GG acknowledge NASA-JPL subcontract No. 1573108 and NRL Base Funds. AS is thankful to the Indian National Science Academy (INSA) for their support under the INSA Senior Scientist Fellowship scheme.

DATA AVAILABILITY

Data sharing is not applicable to this article as no new data were created or analyzed in this study.

[1] K. O. Hill, D. C. Johnson, B. S. Kawasaki, and R. I. MacDonald, *J. Appl. Phys.* **49**, 5098 (1978).
[2] P. Fischer, D. S. Wiersma, R. Righini, B. Champagne, and A. D. Buckingham, *Phys. Rev. Lett.* **85**, 4253 (2000).
[3] Y. Shi, *Phys. Rev. E* **99**, 063212 (2019). [4] B. Liu, J. Goree, T. M. Flanagan, A. Sen, S. K. Tiwari, G. Ganguli, and C. Crabtree, *Phys. Plasmas* **25**, 113701 (2018).
[5] L.-W. Teng, M.-C. Chang, Y.-P. Tseng, and L. I, *Phys. Rev. Lett.* **103**, 245005 (2009).

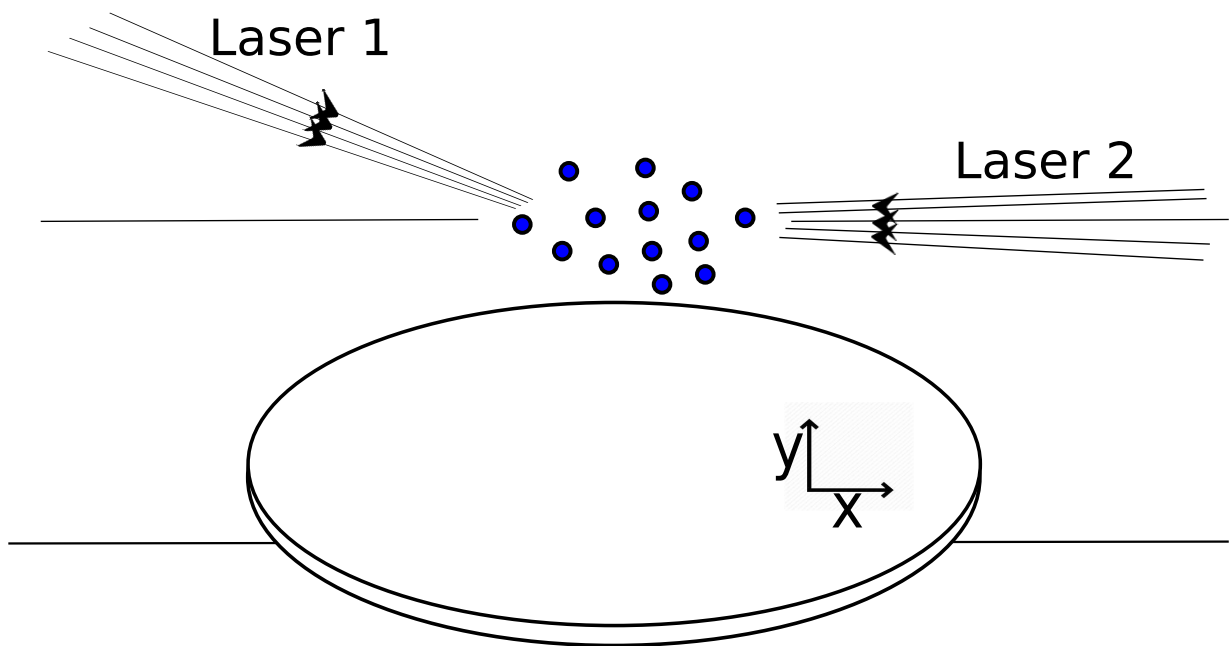
This is the author's peer reviewed, accepted manuscript. However, the online version of record will be different from this version once it has been copyedited and typeset.

PLEASE CITE THIS ARTICLE AS DOI: 10.1063/5.0022482

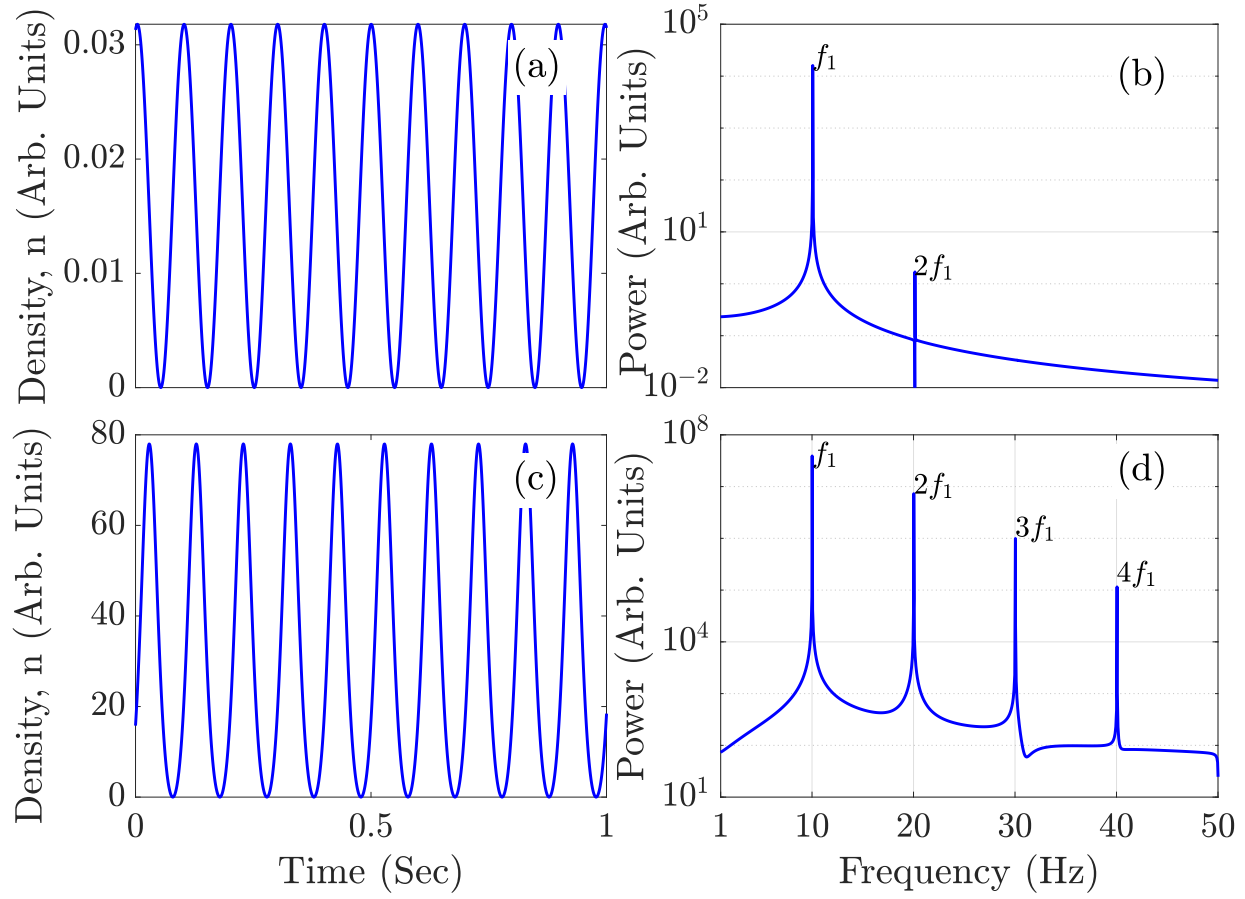
369 [6] A. Homann, A. Melzer, S. Peters, and A. Piel, Phys. Rev. E **56**, 7138 (1997).
370 [7] F. Melandsø, Phys. Plasmas **3**, 3890 (1996).
371 [8] A. Barkan, R. L. Merlino, and N. D'Angelo, Phys. Plasmas **2**, 3563 (1995).
372 [9] J. Heinrich, S.-H. Kim, and R. L. Merlino, Phys. Rev. Lett. **103**, 115002 (2009).
373 [10] T. Deka, A. Boruah, S. K. Sharma, and H. Bailung, Phys. Plasmas **24**, 093706 (2017).
374 [11] S. Nunomura, D. Samsonov, and J. Goree, Phys. Rev. Lett. **84**, 5141 (2000).
375 [12] A. Homann, A. Melzer, S. Peters, R. Madani, and A. Piel, Phys. Lett. A **242**, 173 (1998).
376 [13] V. Nosenko, K. Avinash, J. Goree, and B. Liu, Phys. Rev. Lett. **92**, 085001 (2004).
377 [14] K. Avinash, P. Zhu, V. Nosenko, and J. Goree, Phys. Rev. E **68**, 046402 (2003).
378 [15] W. D. S. Ruhumusiri and J. Goree, Phys. Rev. E **85**, 046401 (2012).
379 [16] T. Deka, B. Chutia, Y. Bailung, S. K. Sharma, and H. Bailung, Plasma Sci. Technol. **22**, 045002 (2020).
380 [17] N. N. Rao, P. K. Shukla, and M. Y. Yu, Planet. Space Sci. **38**, 543 (1990).
381 [18] P. K. Shukla and A. A. Mamun, New J. Phys. **5**, 17 (2003).
382 [19] P. Bandyopadhyay, G. Prasad, A. Sen, and P. K. Kaw, Phys. Rev. Lett. **101**, 065006 (2008).
383 [20] P. Bandyopadhyay, U. Konopka, S. A. Khrapak, G. E. Morfill, and A. Sen, New J. Phys. **12**, 073002 (2010).
384 [21] A. Sen, S. Tiwari, S. Mishra, and P. Kaw, Adv. Space Res. **56**, 429 (2015).
385 [22] S. Jaiswal, P. Bandyopadhyay, and A. Sen, Phys. Rev. E **93**, 041201 (2016).
386 [23] G. Arora, P. Bandyopadhyay, M. G. Hariprasad, and A. Sen, Phys. Plasmas **26**, 093701 (2019).
387 [24] B. Farokhi, P. Shukla, N. Tsintsadze, and D. Tskhakaya, Phys. Lett. A **264**, 318 (1999).
388 [25] G. M. Peradze and N. L. Tsintsadze, Low Temp. Phys. **45**, 103 (2019).
389 [26] D. A. Fogaça, F. S. Navarra, and L. G. Ferreira Filho, Phys. Rev. D **84**, 054011 (2011).
390 [27] Y. C. Mo, R. A. Kishen, D. Feldman, I. Haber, B. Beaudoin, P. G. O'Shea, and J. C. T. Thangaraj, Phys. Rev. Lett. **110**, 084802 (2013).
391 [28] D. Samsonov, A. V. Ivlev, R. A. Quinn, G. Morfill, and S. Zhdanov, Phys. Rev. Lett. **88**, 095004 (2002).
392 [29] S. K. Sharma, A. Boruah, and H. Bailung, Phys. Rev. E **89**, 013110 (2014).
393 [30] H. Leblond, Phys. Rev. A **78**, 013807 (2008).
394 [31] A. Gasch, T. Berning, and D. Jäger, Phys. Rev. A **34**, 4528 (1986).
395 [32] E. F. El-Shamy, Phys. Rev. E **91**, 033105 (2015).
396 [33] A. R. Osborne, Phys. Rev. E **48**, 296 (1993).
397 [34] M. Dingemans, *Water Wave Propagation Over Uneven Bottoms*, Advanced Series on Ocean Engineering (World Scientific, Singapore, 1997).
398 [35] A. H. Salas, Nonlinear Anal. Real World Appl. **12**, 1314 (2011).
399 [36] (2011).

This is the author's peer reviewed, accepted manuscript. However, the online version of record will be different from this version once it has been copyedited and typeset.

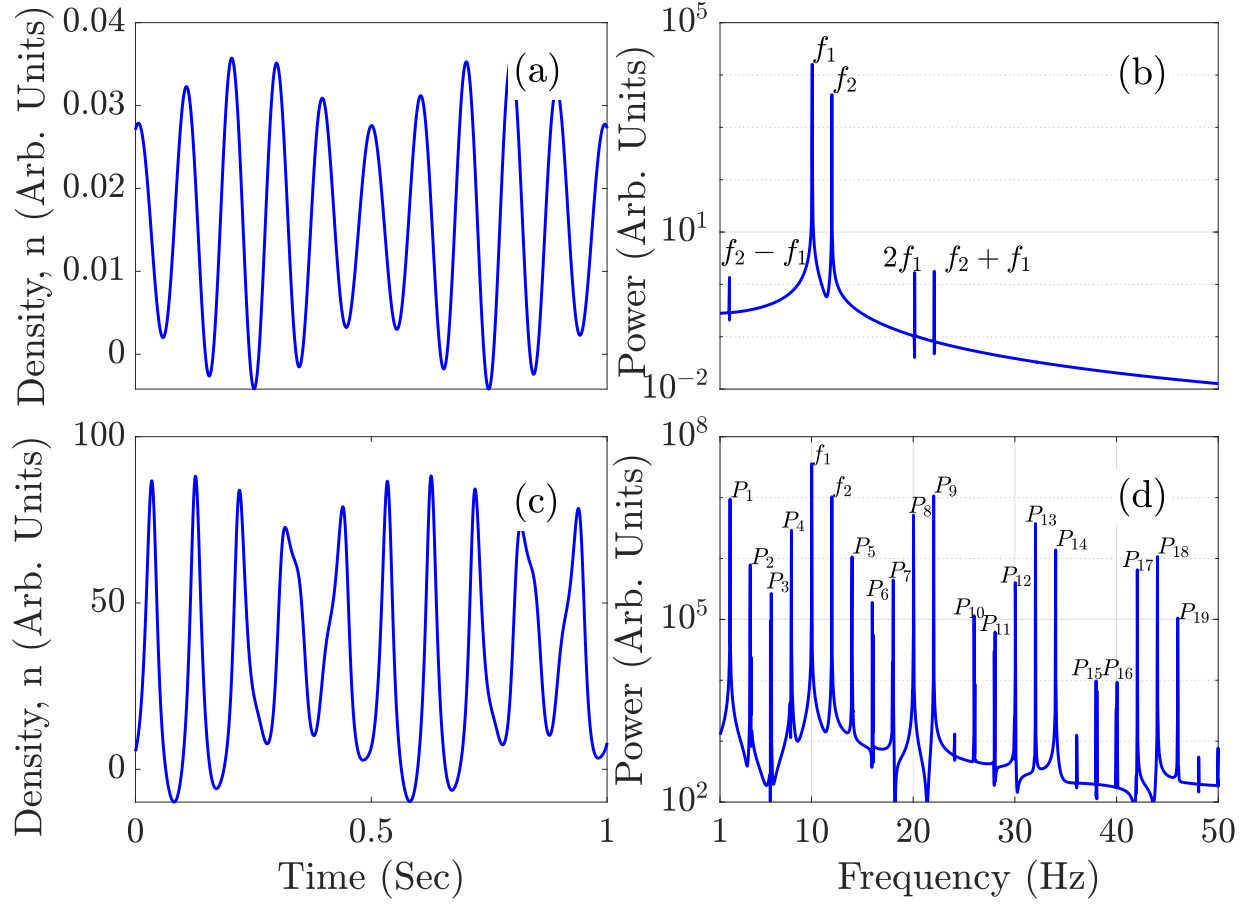
PLEASE CITE THIS ARTICLE AS DOI: 10.1063/5.0022482



This is the author's peer reviewed, accepted manuscript. However, the online version of record will be different from this version once it has been copyedited and typeset.
PLEASE CITE THIS ARTICLE AS DOI: 10.1063/5.0022482



This is the author's peer reviewed, accepted manuscript. However, the online version of record will be different from this version once it has been copyedited and typeset.
PLEASE CITE THIS ARTICLE AS DOI: 10.1063/5.0022482



This is the author's peer reviewed, accepted manuscript. However, the online version of record will be different from this version once it has been copyedited and typeset.

PLEASE CITE THIS ARTICLE AS DOI: 10.1063/5.0022482

